View metadata, citation and similar papers at core.ac.uk
brought to you by CORE
provided by Crossref

Research article Related Commentary, page 593

The DEAD-box RNA helicase Vad1 regulates multiple virulence-associated genes in *Cryptococcus neoformans*

John Panepinto,[1] Lide Liu,[1] Jeanie Ramos,[1] Xudong Zhu,[1] Tibor Valyi-Nagy,[2] Saliha Eksi,[3] Jianmin Fu,[4] H. Ari Jaffe,[1] Brian Wickes,[4] and Peter R. Williamson[1,5]

[1]Section of Infectious Diseases, Department of Medicine, University of Illinois at Chicago College of Medicine, Chicago, Illinois, USA. [2]Department of Pathology, University of Illinois at Chicago Medical Center, Chicago, Illinois, USA. [3]Department of Biology, Loyola University, Chicago, Illinois, USA. [4]Department of Microbiology and Immunology, The University of Texas Health Science Center at San Antonio, San Antonio, Texas, USA. [5]Jesse Brown VA Medical Center, Chicago, Illinois, USA.

The study of fungal regulatory networks is essential to the understanding of how these pathogens respond to host environmental signals with effective virulence-associated traits. In this study, a virulence-associated DEAD-box RNA helicase–encoding gene (*VAD1*) was isolated from a mutant defective in the virulence factor laccase. A Δ*vad1* mutant exhibited a profound reduction in virulence in a mouse model that was restored after reconstitution with WT *VAD1*. Loss of *VAD1* resulted in upregulation of *NOT1*, a gene encoding a global repressor of transcription. *NOT1* was found to act as an intermediary transcriptional repressor of laccase. Vad1 was located within macromolecular complexes that formed cytoplasmic granular bodies in mature cells and during infection of mouse brain. In addition, *VAD1* was shown by in situ hybridization to be expressed in the brain of an AIDS patient coinfected with *C. neoformans*. To understand the role of *VAD1* in virulence, a functional genomics approach was used to identify 3 additional virulence determinants dependent on *VAD1*: *PCK1*, *TUF1*, and *MPF3*, involved in gluconeogenesis, mitochondrial protein synthesis, and cell wall integrity, respectively. These data show that fungal virulence-associated genes are coordinately regulated and that an analysis of such transcriptomes allows for the identification of important new genes involved in the normal growth and virulence of fungal pathogens.

Introduction

The basidiomycetous yeast *Cryptococcus neoformans* has emerged as one of the major causative agents of meningoencephalitis in immunocompromised hosts, such as persons with AIDS, organ transplant recipients, and patients receiving high doses of corticosteroid treatment, although systemic infections can also occur in immunocompetent individuals (1, 2). However, the spectrum of disease in AIDS has been changing with the advent of highly active antiretroviral therapy with the recognition of an immune reconstitution syndrome associated with cryptococcosis (3). As rates of infection have diminished in developed countries, attention is increasingly being focused on the high rates of cryptococcosis in the developing countries of Africa and Asia where cryptococcosis was found to account for an estimated 17% of AIDS-related deaths in one cohort in Uganda (4). *C. neoformans* has been divided into 4 serotypes, A–D, of which A and D cause the vast majority of infections in Europe and the United States (5).

Molecular and immunological studies over the past years have provided numerous insights into the basis of virulence of this yeast. The 3 best-known virulence-associated traits of *C. neoformans* include: (a) its ability to grow at 37°C dependent on calcineurin (6, 7); (b) the presence of a copper-containing laccase that is capable of producing melanin pigments (8, 9); and (c) a high molecular-weight polysaccharide capsule (10–15). In addition, genetic knockout experiments have established the role of a number of other traits required for survival and virulence of *C. neoformans*, including purine metabolism (16), myristylation (17), signal transduction (18–20), α-mating type locus (21), mannitol synthesis (22, 23), phospholipase (24), urease (25), and manosylation activities (26). Despite this extensive repertoire of identified virulence-associated genes, little is known about how the organism regulates pathogenesis by organizing the expression of these genes.

One approach for the study of virulence regulation has been to model cryptococcal virulence on signal transduction pathways evident in the model yeast, *Saccharomyces cerevisiae*. For example, the MAPK pathway has been studied in both serotype A and serotype D *C. neoformans* because of its known role in mating and activation of filamentous growth for food foraging under starvation conditions in *S. cerevisiae*. However, while many of the MAPK members have profound effects on mating in *C. neoformans* (*GPB1*, *STE7*, *STE11*, and *CPK1*), only 2 (*STE12*, *STE20*) have been implicated directly in virulence-related gene regulation, and this was found to be strain dependent (27–29). The variability in the penetrance of this pathway in *Cryptococcus* has led one investigator to propose that *STE12* functions in parallel to the MAPK cascade in this fungus by an additional unknown pathway (27). A second signaling pathway implicated in virulence of *C. neoformans* has been the nutrient-sensing Gα protein cAMP-protein kinase A pathway, although the role of this pathway in virulence also appears to be strain dependent (18, 30, 31).

To identify additional regulatory pathways not evident from the study of model yeasts, we employed random insertional

Nonstandard abbreviations used: RNAi, RNA interference; TIGR, The Institute of Genomic Research; *VAD1*, virulence-associated DEAD-box RNA helicase–encoding gene; YPD, yeast extract–peptone–dextrose.

Conflict of interest: The authors have declared that no conflict of interest exists.

Citation for this article: *J. Clin. Invest.* **115**:632–641 (2005). doi:10.1172/JCI200523048.

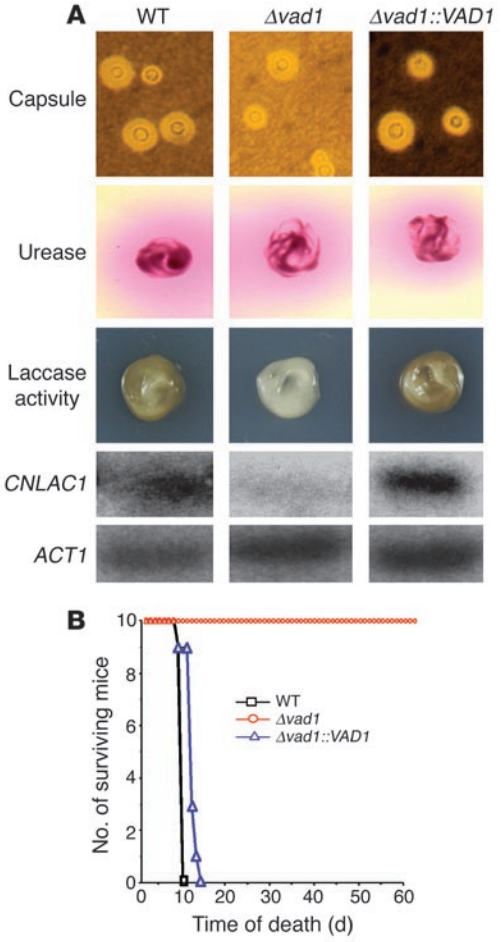

Figure 1
VAD1 mutants show reductions in laccase activity and transcription and markedly attenuated virulence in a mouse model. (**A**) The indicated cells were incubated on malt extract for 5 days at 30°C and examined by India Ink microscopy for analysis of capsule, incubated for 20 minutes on Christensen's media for analysis of urease activity, and inoculated on asparagine agar containing norepinephrine to assay production of melanin pigment by laccase. Transcription of laccase was measured using an 874-bp fragment of *CNLAC1* as previously described (8) from RNA obtained from cells incubated in asparagine media without glucose for 3 hours at 30°C. A PCR-amplified fragment of the *ACT1* gene (68) was used as a control. (**B**) Mice were injected by tail vein (10^6 of the indicated cells), and progress was followed until they were moribund.

mutagenesis and plasmid rescue in *C. neoformans* and screened for mutants defective in the virulence factor laccase. Plasmid recovered by excision from genomic DNA of one such mutant showed that the disrupted gene encoded a member of the RCK/p54 subfamily of RNA DExD/H-box proteins, which was subsequently named virulence-associated DEAD-box RNA helicase-encoding protein (Vad1). Members of this family of proteins have been identified as components of the CCR4-NOT complex, a global regulator of transcription and mRNA stability (32). Further studies showed that *VAD1* is an important regulator of stress response and plays a role in the expression of several new virulence determinants involved in diverse traits, such as stress-responsive growth, salt tolerance, and virulence, each accounting for a portoin of the Δ*vad1* phenotype.

Results and Discussion

Insertional mutagenesis and recovery of a Δ*vad1 mutant of C. neoformans*. A laccase-deficient mutant was produced by insertional mutagenesis using a pMUT8 plasmid derived from a *URA5* transformation marker inserted into pBluescript as described previously (33). A 7-kb plasmid that contained a fragment of the interrupted gene region was rescued from the genomic DNA of the cryptococcal mutant. Through the use of plasmid sequence, the National Center for Biotechnology Information (NCBI) database, and the alignment tool, BLAST, the interrupted gene was found to encode a putative 616 AA polypeptide and to display homology with a conserved subfamily of RNA-binding DExD/H-box proteins referred to as RCK/p54, after the human protein (34). Members within this family include the 485 AA Ste13 of *Schizosaccharomyces pombe* (74% identity, e^{-180}), the 506 AA Dhh1 from *S. cerevisiae* (71% identity, e^{-170}), and a 484 AA human p54 (66% identity, e^{-164}). Members of this class of proteins have been implicated in nuclear functions (35) as well as in modulation of the cytoplasmic mRNA decapping and deadenylation complex (36). The cryptococcal protein is composed of a highly conserved DExD/H-box region of 400 AAs (74% identity to Ste13; 72% identity to Dhh1) and a less conserved glutamine-rich (27%) 200-AA C-terminus (see Supplemental Figure 1; supplemental material available online with this article; doi:10.1172/JCI200523048DS1.). The C-terminus of other proteins of this class are also glutamine-rich (Dhh1-26%; Ste13-12%), but are much shorter (100 AA) than the cryptococcal protein. Differences between sequences of the C-terminus of the cryptococcal protein and those of others of the class may suggest functions specific to the cryptococcal protein. Because of these structural differences, we decided not to name the gene after the *S. cerevisiae* gene, *DHH1*. Rather, because of the association with the virulence factor laccase, the cryptococcal protein was named Vad1.

Phenotypic analysis of virulence-associated traits in VAD1 strains. In addition to typical yeast traits, *C. neoformans* expresses several factors that are involved in its role as a human pathogen and were assessed in the *VAD1* strains. As shown in Figure 1A, laccase activity and transcription were reduced in the Δ*vad1* mutant and were restored after complementation with WT *VAD1*. In contrast, capsule and urease activity were unaffected by the mutation. The *VAD1* strains were next assessed for virulence in a mouse dissemination model because this model was previously used to establish a role for laccase in the virulence of *C. neoformans* (9). Despite the presence of residual laccase activity, the Δ*vad1* strain showed marked attenuation in virulence in this model even after a large inoculum of 10^6 organisms ($P < 0.001$; Figure 1B). The degree of hypovirulence was surprising, given that previous studies of strains completely lacking laccase showed minor residual virulence (9). This suggests that the Δ*vad1* mutant exhibits defects other than laccase expression that impair virulence. Reconstitution of the Δ*vad1* mutant with WT *VAD1* completely restored virulence, confirming that the alteration of virulence was not due to a secondary, unintended mutation.

Phenotypic analysis of RCK/p54-associated traits in VAD1 strains. Analysis of the Δ*vad1* mutant showed that this gene shares traits associated with the RCK/p54 subfamily but also possesses features unique to *C. neoformans*. Growth rates of the mutants in yeast extract–peptone–dextrose (YPD) broth were virtually identical at 30°C and 37°C (doubling time in hours at 30°C: 2.5, 2.5, 2.5; at

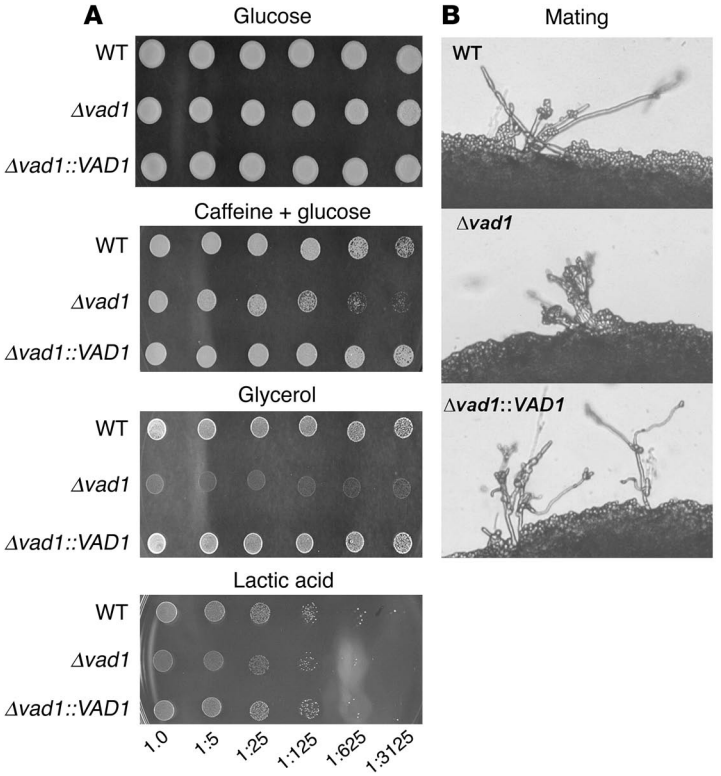

Figure 2
Phenotypic analysis of *VAD1* mutants of *C. neoformans*. (**A**) The indicated strains were diluted to an A_{600} of 1.0, and 1:5 serial dilutions (5 μl) were plated on asparagine media containing the indicated substrates and incubated at 30°C for 3 days. (**B**) Indicated cells were mixed with an isogenic α-mating type strain on proline agar for 1 week at 25°C and observed by microscopy. Magnification, ×100.

37°C: 2.3, 2.5, 2.3 for WT, Δ*vad1*, and Δ*vad*:*VAD1* strains, respectively) and on asparagine salt agar with 2% glucose (Figure 2A), but the Δ*vad1* mutant showed significantly reduced growth on the same agar media supplemented with 8 mM caffeine or when the carbon source was replaced by the nonfermentable substrates glycerol or lactate, with the mutant forming petite colonies on the latter (Figure 2A). The doubling time of the WT and Δ*vad1* mutant in medium containing lactic acid as the sole source of carbon was 8.8 hours (± 1.2) and 12.85 hours (± 0.35) respectively, providing verification of the spot-plate data. In addition to exhibiting increased doubling time, the Δ*vad1* mutant grew to a lower final density (OD_{600} = 0.19) than the WT (OD_{600} = 0.23) in medium supplemented with lactic acid. Reduced growth was also observed in media containing 1M NaCl and 1.8 M sorbitol (data not shown). Sensitivity to salt, sorbitol, and caffeine are indications of a defect in cell wall integrity (32). Cell wall defects and reduced ability to utilize nonfermentable substrates are phenotypes shared by Δ*vad1* mutants and mutants of the *S. cerevisiae* RCK/p54 member *DHH1* (50, 74). However, the Δ*vad1* mutant was different from that of its closest homolog, *S. pombe STE13* (37), in that it retained the ability to mate and produce basidiospores (Figure 2B), although less vigorously than the WT. Reconstitution of the mutant with WT *VAD1* restored all defective phenotypes.

Sizing and cell localization of the VAD1 multiprotein complex. To facilitate immunolocalization of the Vad1 protein, a 10-AA *c-myc* tag was inserted within the WT *VAD1* gene at AA position 58 and used to complement the Δ*vad1* mutant. Proper functioning of the *VAD1–c-myc* construct was verified by restoration of laccase expression in the reconstituted Δ*vad1*:*VAD1*–c-myc strain (Figure 3A, bottom panel). Western blot analysis using a *c-myc* monoclonal antibody showed a single band on SDS-PAGE corresponding to the expected molecular mass of the Vad1 protein (Figure 3A, top panel, lane 2), which was not evident on cell extract from the Δ*vad1* mutant (Figure 3A, top panel, lane 1). Cell extract of cryptococcal cells expressing the *VAD1–c-myc* construct was subjected to gel filtration on a TSK-GEL G6000 (Supelco Chromatography) high-performance liquid chromatography (HPLC) column and analyzed by dot blot hybridization of column fractions. As shown in Figure 3B, comparison of elution profiles of the *c-myc* reactive material to molecular mass standards showed the presence of a large Vad1 multiprotein complex migrating at a size predominately at 0.5–2.0 mDa. The finding of large multiprotein complexes in vitro suggests that the Vad1 protein is part of a large regulatory complex, which is consistent with the functions of other members of the RCK/p54 subfamily. *DHH1*, the *S. cerevisiae* homolog of *VAD1*, has been shown to interact with members of the CCR4-NOT regulatory complex (32).

To determine the cellular localization of Vad1, the Δ*vad1* strain was complemented with a WT *VAD1* fragment containing a C-terminal GFP tag. To mimic WT expression, the construct was expressed under the control of the native *VAD1* promoter and was inserted into the genome as determined by Southern blots of uncut DNA, which localized the construct to genomic DNA (data not shown). Complementation of the Δ*vad1* mutant with the VAD1-GFP construct restored laccase expression, confirming the functionality of the fusion protein (data not shown). During active budding in the presence of glucose, immature daughter cells that did not yet contain nuclei observable by DAPI staining showed accumulation of Vad1 in the cytoplasm, seen as a diffuse fluorescence specific to cells expressing GFP-Vad1 (Figure 3C). Once daughter cells matured and nuclei were observed, Vad1 was consistently found in cytoplasmic locations in structures similar to the recently described P-bodies containing the RCK/p54 submember of *S. cerevisiae* and other gene products involved in transcript stability (38). The cytoplasmic granular appearance of Vad1 was then maintained during glucose starvation, although the granules appeared slightly larger than those of nonstarved mature cells (Figure 3C). Untransformed WT cells showed no specific cellular localization and weak autofluorescence that was evident at multiple wavelengths, whereas Vad1-GFP fluorescence was only visible at GFP-specific wavelengths. Vad1-GFP fluorescence never colocalized with DAPI, which suggests that it does not exhibit nuclear localization, making a role for *VAD1* in nuclear DNA-binding unlikely. This is in contrast to what has been reported for the human homolog p54 (39). While the RNA helicase proteins are numerous and typically have diverse housekeeping functions, the recently described RCK/p54 subfamily appears to have a more restricted, possibly regulatory function (32). It has been proposed that human and mouse p54 RCK/p54 homologs are protooncogenes (39). The *S. cerevisiae* homolog, Dhh1, has been proposed as having a role in transcription due to its genetic and physical interactions with the regulatory CCR4-NOT complex (40, 41). In addition, Dhh1 has also been found to have a role in

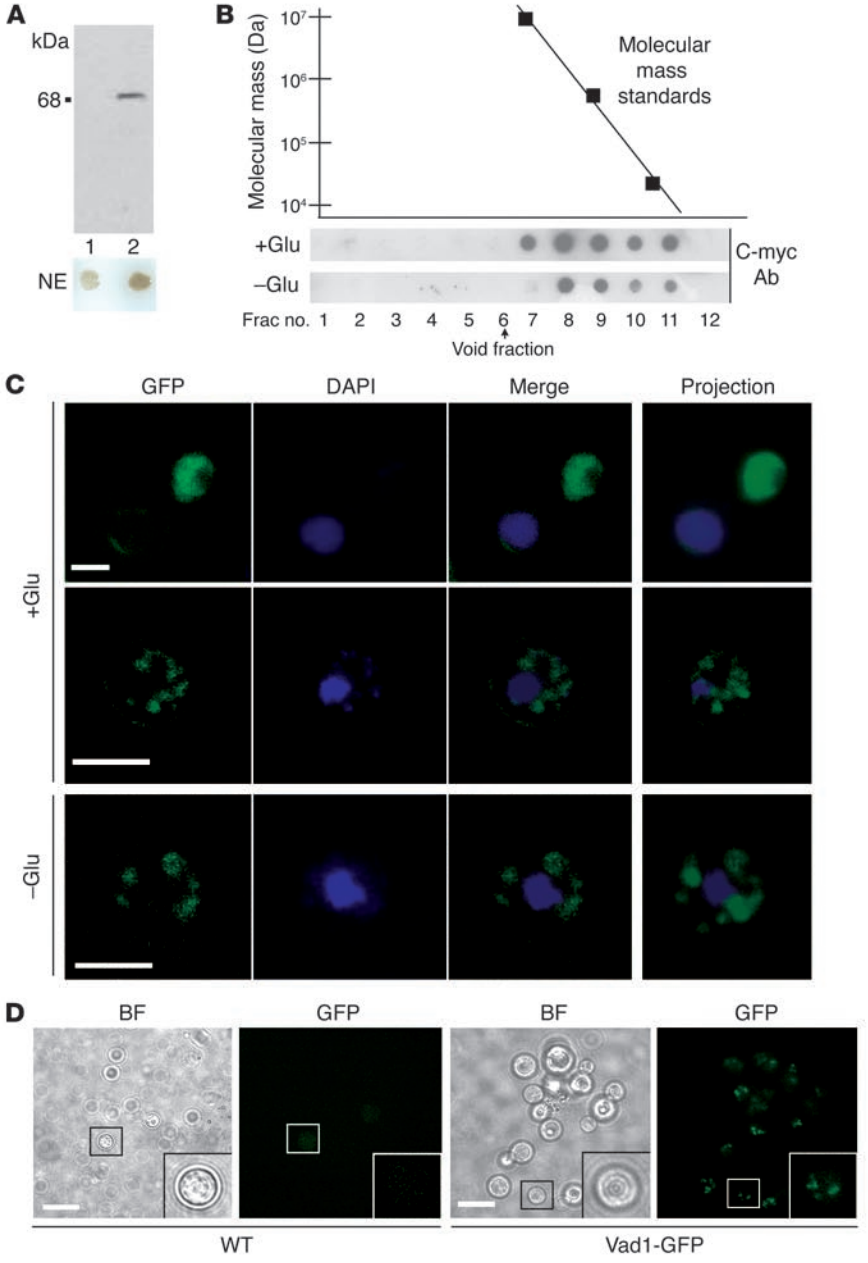

Figure 3
Vad1 is contained within cytoplasmic bodies of high molecular weight in vitro and during neuropathogenesis. (**A**) Top panel: Western blot of cell extract from a Δ*vad1* mutant (lane 1) and a strain expressing a c-myc–tagged Vad1 developed with an anti–c-myc monoclonal antibody (lane 2). Bottom panel: Same strains incubated on asparagine agar containing norepinephrine (NE) for 24 hours. (**B**) Cells were incubated in asparagine media plus or minus glucose (Glu), and cell extracts were subjected to gel filtration chromatography. Fractions (Frac) were denatured by heating and spotted on nitrocellulose and developed with an anti–c-myc monoclonal antibody. (**C**) Cells expressing GFP-tagged Vad1 were incubated under the indicated conditions in vitro and examined by fluorescence microscopy as described in Methods. Scale bars: 5 μm. (**D**) WT cells (left panels) or cells expressing GFP-tagged Vad1 (right panels) were inoculated into mice, recovered from brains, and subjected to fluorescence microscopy. Scale bars: 10 μm. Insets represent higher magnification view of indicated similar-sized cells from the WT- and Vad1-GFP–expressing strains.

transcript stability by physically interacting with and modulating the function of the mRNA decapping complex (36, 38). These data would suggest a role for *VAD1* in cytoplasmic processes such as RNA stability as proposed for yeast Dhh1 (36) rather than a direct role in transcription initiation.

To assess the expression and cellular localization during neuropathogenesis, cells expressing the Vad1-GFP fusion protein were inoculated into mice and subsequently recovered from mouse brains (colony counts from brain at time of sacrifice: 70,600 ± 4,900 cfu/g; $n = 3$). As shown in Figure 3D, cells recovered from mouse brains during infection ($n = 200$) showed expression of Vad1 protein, and all cells were observed to have the granular appearance of mature cells, indicating a predominance of the mature cell type during infection of the mouse brain (right panels). WT cells exhibited only nonspecific autofluorescence (left panels). The observance of predominantly mature cells during brain infection suggests that survival of *C. neoformans* in brains is primarily due to the fungus's resistance to killing by the host rather than by rapid fungal growth and effective host killing.

VAD1 is expressed in brain during human cryptococcal infection. To validate the study of *VAD1* as it relates to virulence, in situ hybridization was performed on sections of human brain infected with *C. neoformans*. The patient was a 42-year-old male who presented with mental status changes and was found to have a CSF cryptococcal antigen of 1:16,348 and a computed tomography (CT) scan suggestive of cerebral edema. The patient was subsequently found to be HIV positive with a $CD4^+$ T cell count of 51 cells/mm^3, and in spite of 1 dose of Amphotericin B, became unresponsive and died. On autopsy, evidence of effacement of the uncus was found consistent with brain herniation. CSF cultures grew *C. neoformans*, and brain sections showed numerous mucicarmine-stained yeasts. Figure 4 shows an autopsy specimen from the cerebral cortex meninges. In situ hybridization was performed with an antisense RNA strand or a sense strand (negative control) of a 579 bp fragment encoding a nonconserved region of the C-terminus and a 3′ untranslated region of *VAD1*. Positive hybridization signal was detected only in sections probed with an antisense probe (Figure 4A). Sections probed with the corresponding sense probe showed no hybridization to yeast forms (Figure 4B). Sections were also stained with mucicarmine specific for *C. neoformans* capsule (Figure 4C) and H&E (Figure 4D). These data demonstrate the expression of *VAD1* during infection of the human brain by *C. neoformans* and provide rationale for fur-

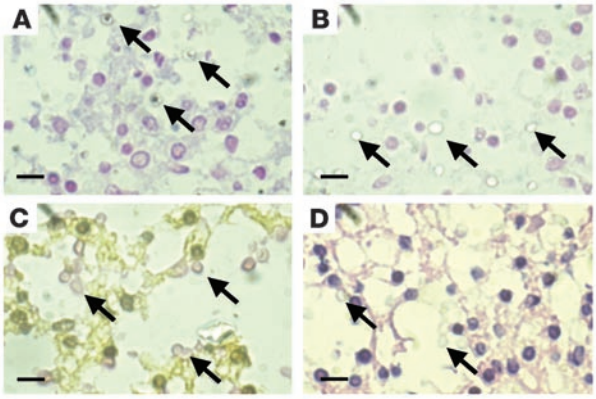

Figure 4
VAD1 is expressed by *C. neoformans* during infection of human brain. (**A**) In situ hybridization of *C. neoformans*–infected brain tissue hybridized with an antisense *VAD1* digoxigenin-labeled RNA probe. Arrows point to alkaline phosphatase–positive yeast cells. (**B**) In situ hybridization of *C. neoformans*–infected brain tissue hybridized with a sense *VAD1* digoxigenin-labeled RNA probe. Arrows point to alkaline phosphatase–negative yeast cells. (**C**) Mucicarmine stain of *C. neoformans*–infected brain tissue. Arrows point to mucicarmine-positive yeast cells. (**D**) H&E stain of *C. neoformans*–infected brain tissue. Arrows point to unstained yeast cells. Scale bars: 10 μm.

ther elucidation of the mechanisms by which loss of *VAD1* results in severe virulence attenuation.

VAD1-dependent genes are essential for normal growth and virulence. Due to the pleiotrophic phenotype of the Δ*vad1* mutant as well as the large degree of virulence attenuation with the mutation, a search was made for other genes, in addition to laccase, that exhibit altered expression in the Δ*vad1* mutant. WT and Δ*vad1* cells were subjected to glucose starvation to derepress laccase expression, and mRNA was compared in duplicate by 24-primer differential display. Four genes, including laccase, showed reduced expression under glucose-starvation conditions, and 1 gene showed increased expression in the Δ*vad1* mutant. The contribution of each to the Δ*vad1* phenotype was assessed by construction of genetically altered strains.

A differential display tag found to be highly enriched in the Δ*vad1* strain relative to the WT exhibited identity to annotated fragment 179.m00475 of The Institute of Genomic Research (TIGR) *Cryptococcus neoformans* database. A BLAST search revealed homology to the *S. cerevisiae NOT1* gene, encoding a global negative regulator of transcription, and the core component of the *CCR4-NOT* complex, of which the *VAD1* homolog, *DHH1*, is also a component. In the WT, the *NOT1* transcript exhibited a moderate level of glucose repression under the conditions tested but was verified to be upregulated in the Δ*vad1* mutant by Northern blot (Figure 5A). To determine the contribution of *NOT1* mRNA accumulation to the Δ*vad1* laccase-deficient phenotype, an episome expressing interfering RNA to the *NOT1* transcript was introduced into the Δ*vad1* mutant. RNA interference (RNAi) was the method of choice since the *S. cerevisiae NOT1* is an essential gene and deletion of any 2 components of the CCR4-NOT complex results in a synthetic lethal phenotype. Expression of *NOT1*-interfering RNA restored laccase activity to the Δ*vad1* mutant as measured on asparagine medium lacking glucose and supplemented with norepinephrine whereas a control plasmid had no effect (Figure 5B, top panel). A Northern blot of total RNA isolated from the WT and the Δ*vad1* mutant containing either the i*NOT1* or iControl plasmid was probed with *NOT1* and *ACT1*, which demonstrated that *NOT1* mRNA is reduced in the Δ*vad1* mutant expressing *NOT1*-interfering RNA (Figure 5B, bottom panel). These data suggest that accumulation of *NOT1* mRNA contributes to the laccase deficiency of the Δ*vad1* mutant and is compatible with roles of other members of the RCK/p54 family in RNA degradation (36). To determine the effect of *NOT1* mRNA accumulation on laccase expression independent of *VAD1* mutation, full-length *NOT1* coding sequence under the control of a *GPD1* promoter was introduced as a transgene into WT *C. neoformans*, creating strain NO20. Overexpression of *NOT1* in the WT resulted in decreased expression of laccase as demonstrated by Northern blot (Figure 5C, top panel) as well as reduction in laccase activity (Figure 5C, bottom panel), which suggest that *NOT1* is a negative regulator of laccase expression in *C. neoformans*.

Next, we proceeded to characterize the 3 transcripts reduced in the Δ*vad1* mutant in parallel to the virulence factor laccase. As shown in Figure 6, 1 fragment was subcloned and sequenced and found to be nearly identical to annotation fragment 162.m02888 of the TIGR *Cryptococcus neoformans* database. A conceptual translation of the annotation fragment resulted in a 607 AA fragment having homology to *PCK1* of *S. cerevisiae* (65% identity to NP013023). *PCK1* encodes the enzyme phosphoenolpyruvate carboxykinase, which catalyzes the only irreversible step in gluconeogenesis and is a major regulatory checkpoint for the control of gluconeogenesis (42, 43). Targeted knockout strains of *PCK1* were constructed and confirmed by Southern blots digested with *BamHI*/*Kpn*I and hybridized with a *PCK1* fragment (Figure 6B; WT: 8.0, 6.0, 1.1 kb; Δ*pck1*: 8.0, 6.0 kb). The Δ*pck1* mutant was found to show normal growth on glucose-containing media (Figure 6C, upper panel), but showed reduced growth on the 3-carbon substrate lactate (Figure 6C, lower panel), similar to that shown by the Δ*vad1* mutant. Growth in YPD and asparagine liquid with 2% glucose at 37°C showed identical rates (doubling times — YPD: 2.5, 2.5; 2% glucose/asparagine: 4.0 and 3.9 hours for WT

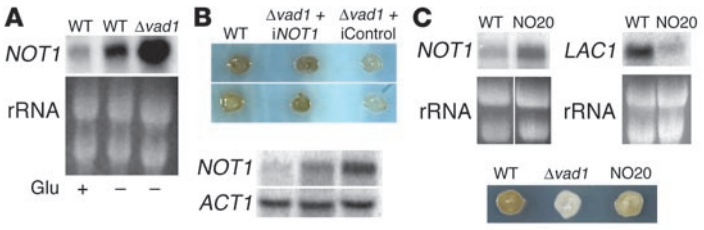

Figure 5
Increased abundance of *NOT1* mRNA, due to deletion of *VAD1* or constitutive overexpression of *NOT1*, represses laccase expression. (**A**) Northern blot analysis of RNA from the indicated cells incubated for 3 hours in asparagine media with or without glucose. (**B**) Top panel: cells of the WT or the Δ*vad1* mutant transformed with the *NOT1* RNAi construct or control plasmid incubated for 8 hours on norepinephrine agar. Bottom panel: Northern blot demonstrating *NOT1* mRNA abundance in the WT strain and the Δ*vad1* mutant transformed with either the *NOT1* RNAi construct or the control plasmid. Actin hybridization is included as a loading control. (**C**) Top panels: Northern analysis of WT- and *NOT1*-overexpressing strain (NO20) incubated for 3 hours in asparagine media without glucose, probed with *NOT1* (left panel) and *LAC1* (right panel). Bottom panel: The WT-, Δ*vad1* mutant–, and *NOT1*-overexpressing strain incubated on norepinephrine agar.

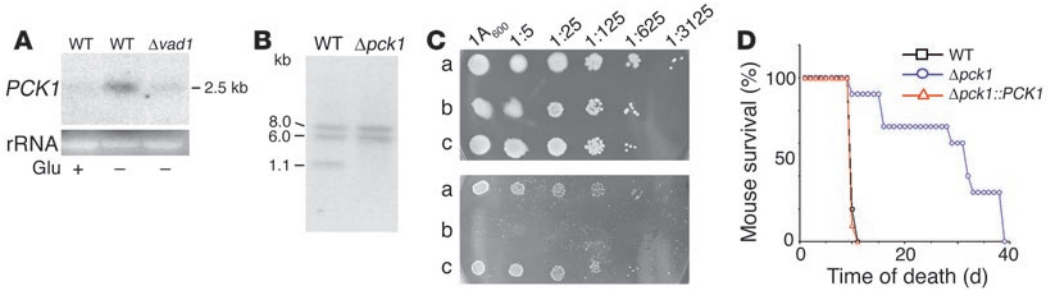

Figure 6
Expression of *PCK1* is dependent on *VAD1*. Deletion of *PCK1* results in defective growth on lactic acid, normal growth on glucose, and attenuated virulence. (**A**) Northern blot analysis of RNA from the indicated cells incubated for 3 hours in asparagine media with or without glucose. (**B**) Southern blot analysis of DNA of the indicated cells digested with *BamH*I and *Kpn*I, hybridized with a fragment of *PCK1*. (**C**) Cells of the WT (a), Δ*pck1* mutant (b), or complemented Δ*pck1*mutant (c) grown on asparagine agar (pH 6.5) containing either 2% glucose (top panel) or 2% lactic acid (bottom panel). (**D**) Survival plot of mice injected with 10^6 CFU of the indicated strains. Mice were sacrificed when moribund.

and Δ*pck1* strains, respectively). Laccase activity was unaffected by the Δ*pkc1* mutation (data not shown). As shown in Figure 6D, the Δ*pck1* mutant was found to be markedly less virulent than WT cells ($P < 0.001$) even at a large inoculum (1×10^6 cells), with restoration of virulence with *PCK1* complementation, showing the importance of this enzyme during infection.

The finding of a role for an RCK/p54 protein in the regulation of *PCK1* has not, to our knowledge, been reported previously and suggests an additional regulatory pathway for this enzyme in addition to the cAMP and Mig-1–dependent pathways previously proposed from studies in *S. cerevisiae* (43). Furthermore, establishment of a role for *PCK1* in cryptococcal virulence provides insights into the pathogenesis of cryptococcal infections. Gluconeogenesis is the pathway for biomass production during periods of glucose deprivation. This anabolic pathway utilizes either 3-carbon fragments such as lactate or 2-carbon fragments such as acetate produced by the glyoxylate shunt pathway and would be expected to be active in environments having low glucose, such as is typical in the brain during cryptococcal meningoencephalitis (44). Recently, the glyoxylate shunt pathway, which utilizes 2-carbon fragments, has been shown to be dispensable for the virulence of *C. neoformans* (45). In combination with this study, the finding that *PCK1* is required for virulence of *C. neoformans* suggests that 3-carbon substrates such as lactate rather than 2-carbon fragments may be preferred for biomass production during infection. Indeed, while lactic acid is produced during fungal meningitis (46), spectroscopy studies have shown a preponderance of the 2-carbon substrate, acetate, during cryptococcal brain infections (47). The accumulation of acetate and consumption of lactate may be due to an inability of the pathogen to optimally utilize acetate by the glyoxylate pathway that is induced only late in infection (45), whereas lactate is successfully consumed and converted into biomass during infection through the gluconeogenic pathway.

The next transcript reduced in the Δ*vad1* mutant was found to be nearly identical to annotation fragment 177.m03152 from the TIGR *Cryptococcus neoformans* database, which is predicted to encode a 480-AA fragment exhibiting 65% identity to *TUF1* from *S. cerevisiae* (NP014830.1). *TUF1* is a nuclear-encoded elongation factor required for translation of mitochondrial proteins; it typically shows reduced growth on all media, especially nonfermentable substrates such as glycerol (48). *TUF1* mRNA abundance was reduced in the Δ*vad1* mutant under both glucose repressed and derepressed conditions (Figure 7A). The *TUF1* transcript, unlike those of *PCK1* and laccase, is not glucose repressible, which suggests that modulation of transcription by *VAD1* is not limited to glucose repressible genes. Attempts to produce a knockout of the cryptococcal *TUF1* were unsuccessful in spite of analysis of approximately 1000 transformants, so RNAi was used to assess the growth phenotypes after *TUF1* transcription inhibition. As shown in Figure 7B, suppression of *TUF1* by RNAi resulted in a reduction of growth under all conditions, including in the presence of glucose, and caused a severe growth reduction on glycerol, consistent with the growth reduction on this nonfermentable substrate demonstrated by the Δ*vad1* mutant. Reduction of *TUF1* expression by RNAi had no effect on laccase expression, which suggests that the reduction of *TUF1* mRNA levels in the Δ*vad1* mutant does not contribute to the laccase-deficient phenotype. The severe impairment of normal growth exhibited by the strains expressing *TUF1*-interfering RNA would most likely result in decreased virulence and was not tested further.

Expression of genes encoded by mitochondrial DNA is essential for oxidative phosphorylation and hence for a large part of ATP production in a cell. The importance of mitochondrial functions has been demonstrated in other cryptococcal studies, in which deletion of a mitochondrial gene encoding the alternative oxidase of mitochondria resulted in defects in tolerance to the stress environment in macrophages and attenuation in cryptococcal virulence (49). *TUF1* regulation by *VAD1* thus suggests a novel pathway for the regulation of mitochondrial functions of eukaryotes in general and fungal pathogens in particular.

The final transcript reduced in the Δ*vad1* mutant is nearly identical to annotation fragment 184.m04573, which is predicted to encode a 416 AA polypeptide. The predicted protein contained a putative hydrophobic leader sequence and glycosyl phosphatidylinositol anchor site and was found to have 40% serines with a ser/thr-rich carboxyterminus (AA 321–396), properties also possessed by a class of cryptococcal mannoproteins recently described as having T cell stimulatory properties (50, 51). Because of these structural similarities to the 2 previous characterized proteins and a lack of a homolog in other organisms as determined by a BLAST analysis of the NCBI database, the gene was named after this class of proteins: mannoprotein of *Filobasidiella neoformans* number 3 (*MPF3*). As shown in Figure 8A, *MPF3* exhibited glucose repression and showed reduced expression in the Δ*vad1* mutant (50% ± 5%), but this reduction was not as marked as that

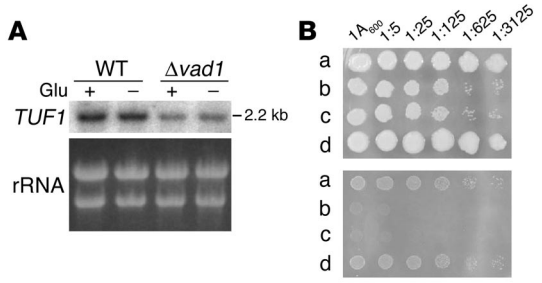

Figure 7
TUF1 is dependent on *VAD1*, and Δ*tuf1* mutants show defective growth on glucose or glycerol. (**A**) Northern blot analysis of RNA from the indicated cells incubated for 3 hours in asparagine media with or without glucose. (**B**) WT cells (a) or cells transformed with the *TUF1* RNAi construct (b and c) or an identical construct containing only the sense strand of the *TUF1* RNAi construct (d) at the indicated dilutions were grown on asparagine agar (pH 6.5) containing either 2% glucose (top panel) or 2% glycerol (bottom panel).

observed for laccase, *PCK1*, or *TUF1*. Deletion of *MPF3* was confirmed by Southern blot (Figure 8B) and resulted in a subtle yellow discoloration of the strains but no observable difference in growth in glucose or glycerol, and the growth rate in 10% human serum was nearly identical to that of the WT and complemented strain (doubling times — WT: 2.7 ± 0.05 hours; Δ*mpf3*: 2.7 ± 0.06 hours; Δ*mpf3:MPF*: 2.6 ± 0.16 hours). No effect on laccase activity was seen in the Δ*mpf3* mutant (data not shown). However, a marked growth defect was observed when the Δ*mpf3* mutant was grown on media containing 1M NaCl or 1.8 M sorbitol (Figure 8C), suggesting a defect in cell wall integrity (32) that was also exhibited by the Δ*vad1* mutant. Injection of mice with a large inoculum (10^6) did not result in a significant alteration in survival of mice (data not shown), but injection of a smaller inoculum (10^3) did result in attenuation of virulence in a mouse model (Figure 8D; $P < 0.01$). These data show a role for *MPF3* in tolerance to osmotic and salt stress and suggest that *MPF3* contributes to the virulence of *C. neoformans*.

The categories of target genes dependent on *VAD1* expression appear remarkable in their wide spectrum of activity in cellular functions. However, all appear to have a role during exposure to stress, implicating *VAD1*-dependent regulation in the cellular stress response. In the mammalian host during pathogenesis, the organism is subjected to a wide variety of cellular stresses (52). As an opportunistic pathogen, *C. neoformans* most likely evolved its stress-regulatory pathways to maximize its chances for survival within its environmental niche, which includes the hollows of trees and occasional encounters with pathogenic amoeba (53, 54). However, the response to environmental stress, mediated by evolved regulatory networks, has also proven effective protection against the mammalian host defense. For example, the *VAD1*-dependent protein laccase is a cell wall enzyme that acts during pathogenesis in the brain to convert dopamine to immunomodulatory products and to neutralize the active iron form within macrophages (55, 56). However, in the hollows of trees, laccase may be considered a foraging enzyme, having a role in lignin degradation for the breakdown of wood (53, 57). Similarly, the induction of *PCK1* that is required for biomass production during glucose starvation in trees can allow utilization of lactic acid produced by host cell macrophages during infection. In addition, *TUF1*, as a required gene involved in the production of mitochondrial proteins, plays a role in efficient ATP generation from oxidative versus fermentative growth (58) that is essential for normal growth in host cells as well as in wooded environments. Finally, *MPF3*, required for protection against osmotic and ionic stress, perhaps during dehydration of the environment, can also serve to protect the pathogen during infection. The combined effects of reduced transcription of these important genes in the Δ*vad1* mutant undoubtedly contribute to the marked attenuation in virulence of the regulatory mutant. These studies are, to our knowledge, the first functional genomics studies of a *C. neoformans* transcriptome and demonstrate the utility of investigating virulence-associated transcriptomes for the identification of new virulence factors in fungal pathogens. Furthermore, identification of virulence-associated master regulators such as Vad1 may allow the pharmacological targeting of multiple virulence phenotypes simultaneously, thus providing more effective methods for the control and prevention of cryptococcosis.

Methods

Insertional mutagenesis of C. neoformans and plasmid rescue of pMUT8 from laccase-deficient mutants. A method of insertional mutagenesis was performed using a linearized plasmid pMUT8 as described previously (33). One mutant with a single genomic insertion of pMUT8 (confirmed by Southern blot) and

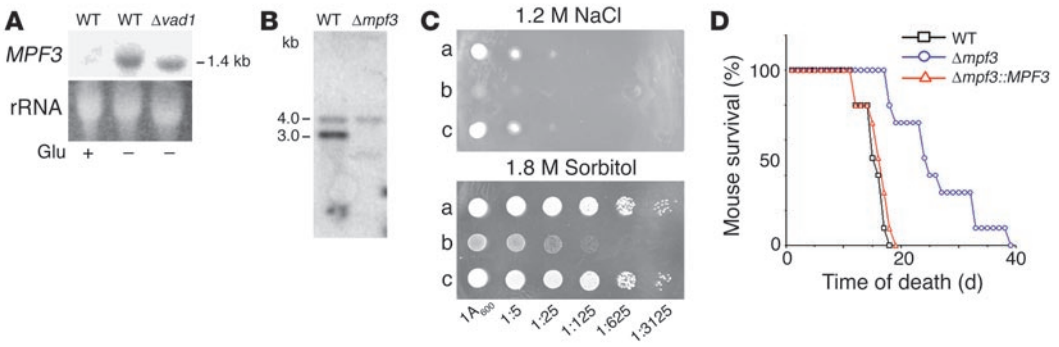

Figure 8
WT *MPF3* transcription is dependent on *VAD1*, and Δ*MPF3* mutants show defective growth on high salt or sorbitol and display attenuated virulence. (**A**) Northern blot analysis of RNA from the indicated cells incubated for 3 hours in asparagine media with or without glucose. (**B**) Southern blot analysis of DNA of the indicated cells digested with *Bgl*II and *Eco*RI, hybridized with a fragment of *MPF3*. (**C**) Cells of the WT (a), Δ*mpf3* mutant (b), or complemented Δ*mpf3* mutant (c) grown on asparagine agar (pH 6.5) containing either 1.2 M NaCl or 1.8 M sorbitol. (**D**) Survival plot of mice injected with 10^3 CFU of the indicated strains. Mice were sacrificed when moribund.

reduced laccase activity was chosen for further investigation. To rescue the inserted pMUT8, genomic DNA was prepared and digested with *Nde*I to excise the insertional plasmid from genomic DNA as previously described (33). A 7-kb insertional plasmid containing the flanking region of a disrupted gene was obtained. Automated sequencing of the plasmid was performed by standard methods (33). Sequences from both sides of the insertional plasmid were used to design oligonucleotide primers (C53T, C53U5) to amplify a 500-bp fragment from H99 genomic DNA using standard PCR methods.

Generation of VAD1 cDNA and genomic clones and complementation of a mutant strain Δvad1. The 500-bp PCR fragment amplified from H99 genomic DNA was used to screen a previously constructed H99 cDNA library (33) by standard techniques. Clone pcVAD1 contained the largest insert and was sequenced from both strands. Genomic and cDNA sequences were aligned and have been submitted to the GenBank database under accession number AY654620. The 2.5-kb fragment of the cDNA clone was radiolabeled to isolate a 4.5-kb genomic DNA allele (clone pgVAD1) from an H99 genomic library generated in a Lambda ZAP Express vector (Stratagene) according to the manufacturer's instructions. To complement the Δ*vad1* mutant, a 2-kb hygromycin B resistant gene was fused with *Cla*I-restricted plasmid pgVAD1 to generate p*VAD1/HgR*, which was transformed into strain Δ*vad1* by electroporation as described (59).

Sizing of epitope-tagged Vad1 by HPLC gel filtration. To construct the *c-myc–VAD1* fusion, 2 oligonucleotides containing a *Stu*I site encoding the sequence EQKLISEEDL were ligated to the complementary site within plasmid p*VAD1/HgR* to generate p*VAD1*/HgR-myc. Correct insertion of the *c-myc* tag was confirmed by sequencing. The construct was digested with *Nhe*I and *Pvu*II to remove the plasmid vector and was transformed into a Δ*vad1* mutant by electroporation. Transformants were selected on hygromycin B–containing medium, confirmed as having the construct inserted by Western blot of whole-cell extracts, and tested for restoration of laccase expression on norepinephrine agar as previously described (33). The *c-myc–VAD1* complemented strain was then grown on YPD media, washed twice with sterile distilled water, and incubated for 3 hours at 30°C in asparagine salts either with 2% glucose or without; cell extracts were subjected to gel filtration on a TSK-GEL G6000 (Supelco Chromatography) HPLC column as described in Supplemental Methods.

Cellular localization of epitope-tagged Vad1 by deconvolution immunomicroscopy. A PCR-amplified fragment of *VAD1* containing *VAD1* promoter elements was inserted upstream of a pBluescript cassette (Stratagene), consisting of a GC-rich GFP (60), an EF1α cryptococcal terminator sequence, and a 1.3-kb fragment of *URA5* previously described (33), and was used to complement the Δ*vad1* mutant to produce strain VGFP-1. VGFP was grown on YPD for 2 days, then inoculated into asparagine liquid containing 2% glucose or identical media without glucose, incubated at 30°C for 3 hours, and prepared for immunofluorescence microscopy as previously described (61). To enable identification of the expression and cellular location of the Vad1 protein during neuropathogenesis, mice were inoculated with 10^5 cells of either WT *C. neoformans* or the GFP-Vad1–expressing strain VGFP-1. Mice were monitored for 2 weeks, after which they were sacrificed by CO_2 narcosis. Brains were immediately removed and sectioned longitudinally. One half of the brain was homogenized and cultured for colony counts and the other half homogenized in ice-cold phosphate-buffered saline and subjected to sucrose-gradient centrifugation for 20 minutes at 4°C to separate *C. neoformans* cells from brain tissue as previously described (62), then subjected to fluorescence microscopy as above.

In situ hybridization. The method of Ausubel et al. (63) was used. Briefly, formaldehyde-fixed tissue was sectioned (4 micron sections), dewaxed with xylene, and rehydrated. A 579-bp *Sac* I-*EcoR* I fragment of the *VAD1* cDNA was subcloned into pBluescript SK (Stratagene), then transcribed in vitro using T7 polymerase and NTPs and labeled with U-digoxigenin according to the manufacturer's instructions (Roche Diagnostics Corp.). The tissue section was subjected to RNA denaturation with sequential washes with 0.2 N HCl, then washed twice with SSC at 70°C, followed by blocking with buffer containing iodoacetamide and N-ethylmaleimide and dehydration. Serial sections were then hybridized with either sense or antisense probes prepared as described above at 50°C overnight, then washed at the same temperature in RNAse-free buffer. Slides were then incubated with a second alkaline phosphatase–conjugated secondary antibody overnight at 4°C, washed, and visualized with 5-bromo,4-chloro,3-indolylphosphate/nitroblue tetrazolium substrate as described in ref. 64. This was followed by staining with Fast Red (Sigma-Aldrich).

Deletion of the PCK1, TUF1, and MPF3 genes in C. neoformans. Constructs for the deletion of *PCK1*, *TUF1*, and *MPF3* consisted of the 1.3-kb *URA5* selectable marker flanked by approximately 500 bp of genomic sequence homologous to the regions upstream and downstream of the coding sequence for each gene. Each construct was transformed into H99FOA as described previously (9). Transformants were screened for homologous recombination by PCR followed by Southern blot verification. A detailed description of the construct design and screening for each gene is included in Supplemental Methods.

RNAi suppression of *TUF1* was performed after the method of Liu et al. (65) using a plasmid derived from pPM8 (66). Briefly, *TUF1* was PCR amplified from a H99 cDNA mass-excised library as previously described (33), using primers TUF1-3114SR and TUF1-3657AX and ligated downstream of the *ACT1* promoter with a linker fragment consisting of a 500–bp PCR-amplified fragment of intron I of *CNLAC1* generated from a *CNLAC1* genomic clone (plasmid p5.1) (8) using primer INTRON-XhoS and INTRON-XhoA to produce plasmid EF-TU7A. EF-TU7A was linearized and transformed into H99FOA and selected on minimal media. Control strains were transformed with the identical plasmid EF-TU7B, which contained only one copy of *TUF1* without a second antisense fragment. A similar plasmid was constructed for suppression of *NOT1* using primers iNOT-F-RI and iNOT-R-Xh. For overexpression of *NOT1*, the full-length *NOT1* coding sequence with a C-terminal *c-myc* tag was PCR amplified with primers FL-NOT-F-Xb and mycNOT-R-Nt, then cloned downstream of the *GPD1* promoter and upstream of the *TRP1* terminator in pSL1180 (Amersham Biosciences) containing the hygromycin resistance cassette. The construct was linearized with *Spe*I and *Vsp*I and transformed into H99 by electroporation. Transformants were selected on YPD with hygromycin, and genomic insertion of the construct was verified by Southern blotting of uncut genomic DNA.

Differential display. Total RNA was isolated from WT (H99) and Δ*vad1* strains (8) under the following conditions: Cells were grown in YPD broth at 30°C to mid-log phase with absorbance of 0.5–0.6 at 600nm. Cells were subsequently derepressed in asparagine medium without glucose (1g/l asparagine, 0.1g/l MgSO4, 10mM sodium phosphate, pH 6.5) at 30°C for 3 hours. Differential display analysis was performed on both strains using 24 primer sets per the manufacturer's instructions (GenHunter). A BLAST search of the sequence (http://www.ncbi.nlm.nih.gov/blast/) from recovered fragments was performed against the TIGR *Cryptococcus neoformans* genome database (http://www.tigr.org/tdb/e2k1/cna1/) to identify the putative open reading frames of the subcloned cryptococcal genomic fragments.

Virulence factor expression, growth rate, mating, and virulence studies. Capsule formation was assessed using methods previously described (33). Urease production was measured by incubation of cells on Christensen's agar (25), and the method of Liu et al. (55) was used to measure laccase activity. Growth rate in liquid media was measured according to Salas et al. (9). Mating was conducted on sucrose proline media as described (67). Virulence studies were conducted according to a protocol using a previously described mouse meningoencephalitis model (9). Animal studies were

approved by the University of Illinois at Chicago Animal Care Committee. Studies involving human tissue were approved by the University of Illinois at Chicago Office for the Protection of Research Subjects and the Institutional Review Board (protocol #2004-0600).

Statistics. Statistical significance of mouse survival times was assessed by Kruskall-Wallis analysis (ANOVA on Ranks). Pairwise analyses were performed post hoc by using Dunn's procedure. Intensity of signals from Northern blot analyses was determined by densitometry using the STORM 860 phosphorimager (Amersham Biosciences).

Acknowledgments

This work was supported, in part, by United States Public Health Service grants NIH AI49371 and AI45995 (to P.R. Williamson), National Research Service Award NIH 1F32AI062124-01 (to J. Panepinto), and an American Heart Association fellowship (to X. Zhu). We would like to acknowledge GenHunter for technical assistance with differential display and Lofstrand Labs Ltd. for technical assistance with in situ hybridization. We also thank TIGR (supported by NIH grant 1 UO1 AI48594-01) and the Fungal Genomic Initiative for preliminary sequence information for the *C. neoformans* genome.

Received for publication August 16, 2004, and accepted in revised form December 14, 2004.

Address correspondence to: John Panepinto, Room 881, m/c 735, 808 South Wood Street, Chicago, Illinois 60612, USA. Phone: (312) 996-8068. Fax: (312) 996-5704. E-mail: panepijc@uic.edu.

1. Casadevall, A., and Perfect, J.R. 1998. *Cryptococcus neoformans*. ASM Press. Washington, D.C., USA. 541 pp.
2. Bichile, L., Gokhale, Y., Sridhar, V., and Gill, N. 2001. Disseminated cryptococcal infection in immune competent patients. *J. Assoc. Physicians India.* **49**:377–378.
3. Jenny-Avital, E., and Abadi, M. 2002. Immune reconstitution cryptococcosis after initiation of successful highly active antiretroviral therapy. *Clin. Infect. Dis.* **35**:e128–e133.
4. French, N., et al. 2002. Cryptococcal infection in a cohort of HIV-1-infected Ugandan adults. *AIDS.* **16**:1031–1038.
5. Mitchell, T.G., and Perfect, J.R. 1995. Cryptococcosis in the era of AIDS--100 years after the discovery of *Cryptococcus neoformans*. *Clin. Microbiol. Rev.* **8**:515–548.
6. Alspaugh, J.A., Cavallo, L.M., Perfect, J.R., and Heitman, J. 2000. RAS1 regulates filamentation, mating and growth at high temperature of *Cryptococcus neoformans*. *Mol. Microbiol.* **36**:352–365.
7. Odom, A., et al. 1997. Calcineurin is required for virulence of *Cryptococcus neoformans*. *EMBO J.* **16**:2576–2589.
8. Williamson, P.R. 1994. Biochemical and molecular characterization of the diphenol oxidase of *Cryptococcus neoformans*: identification as a laccase. *J. Bacteriol.* **176**:656–664.
9. Salas, S.D., Bennett, J.E., Kwon-Chung, K.J., Perfect, J.R., and Williamson, P.R. 1996. Effect of the laccase gene CNLAC1, on virulence of *Cryptococcus neoformans*. *J. Exp. Med.* **184**:377–386.
10. Chang, Y.C., and Kwon-Chung, K.J. 1994. Complementation of a capsule-deficient mutation of *Cryptococcus neoformans* restores its virulence. *Mol. Cell. Biol.* **14**:4912–4919.
11. Chang, Y.C., Wickes, B.L., and Kwon-Chung, K.J. 1995. Further analysis of the *CAP59* locus of *Cryptococcus neoformans*: structure defined by forced expression and description of a new ribosomal protein-encoding gene. *Gene.* **167**:179–183.
12. Chang, Y.C., Penoyer, L.A., and Kwon-Chung, K.J. 1996. The second capsule gene of *Cryptococcus neoformans*, *CAP64*, is essential for virulence. *Infect. Immun.* **64**:1977–1983.
13. Chang, Y.C., et al. 1997. Structure and biological activities of acapsular *Cryptococcus neoformans* 602 complemented with the *CAP64* gene. *Infect. Immun.* **65**:1584–1592.
14. Chang, Y.C., and Kwon-Chung, K.J. 1998. Isolation of the third capsule-associated gene, *CAP60*, required for virulence in *Cryptococcus neoformans*. *Infect. Immun.* **66**:2230–2236.
15. Janbon, G., Himmelreich, U., Moyrand, F., Improvisi, L., and Dromer, F. 2001. Cas1p is a membrane protein necessary for the o-acetylation of the *Cryptococcus neoformans* capsular polysaccharide. *Mol. Microbiol.* **42**:453–467.
16. Perfect, J.R., Toffaletti, D.L., and Rude, T.H. 1993. The gene encoding phosphoribosylaminoimidazole carboxylase (*ADE2*) is essential for growth of *Cryptococcus neoformans* in cerebrospinal fluid. *Infect. Immun.* **61**:4446–4451.
17. Lodge, J.K., Jackson-Machelski, E., Toffaletti, D.L., Perfect, J.R., and Gordon, J.I. 1994. Targeted gene replacement demonstrates that myristoyl-CoA: protein N-myristoyltransferase is essential for viability of *Cryptococcus neoformans*. *Proc. Natl. Acad. Sci. U. S. A.* **91**:12008–12012.
18. Alspaugh, J.A., Perfect, J.R., and Heitman, J. 1997. *Cryptococcus neoformans* mating and virulence are regulated by the G-protein alpha subunit *GPA1* and cAMP. *Genes Dev.* **11**:3206–3217.
19. Chang, Y.C., Wickes, B.L., Miller, G.F., Penoyer, L.A., and Kwon-Chung, K.J. 2000. *Cryptococcus neoformans STE12*alpha regulates virulence but is not essential for mating. *J. Exp. Med.* **191**:871–882.
20. Alspaugh, J.A., et al. 2002. Adenylyl cyclase functions downstream of the G-alpha protein GPA1 and controls mating and pathogenicity. *Eukaryotic Cell.* **1**:75–84.
21. Kwon-Chung, K.J., Edman, J.C., and Wickes, B.L. 1992. Genetic association of mating types and virulence in *Cryptococcus neoformans*. *Infect. Immun.* **60**:602–605.
22. Chaturvedi, V., Flynn, T., Niehaus, W.G., and Wong, B. 1996. Stress tolerance and pathogenic potential of a mannitol mutant of *Cryptococcus neoformans*. *Microbiology.* **142**:937–943.
23. Suvarna, K., Bartiss, A., and Wong, B. 2000. Mannitol-1-phosphate dehydrogenase from *Cryptococcus neoformans* is a zinc-containing long-chain alcohol/polyol dehydrogenase. *Microbiology.* **146**:2705–2713.
24. Cox, G.M., et al. 2001. Extracellular phospholipase activity is a virulence factor for *Cryptococcus neoformans*. *Mol. Microbiol.* **39**:166–175.
25. Cox, G.M., Mukherjee, J., Cole, G.T., Casadevall, A., and Perfect, J.R. 2000. Urease as a virulence factor in experimental cryptococcosis. *Infect. Immun.* **68**:443–448.
26. Wills, E.A., et al. 2001. Identification and characterization of the *Cryptococcus neoformans* phosphomannose isomerase-encoding gene, *MAN1*, and its impact on pathogenicity. *Mol. Microbiol.* **40**:610–620.
27. Davidson, R., Nichols, C., Cox, G., Perfect, J., and Heitman, J. 2003. A MAP kinase cascade composed of cell type specific and non-specific element controls mating and differentiation of the fungal pathogen *Cryptococcus neoformans*. *Mol. Microbiol.* **49**:469–485.
28. Yue, C., et al. 1999. The *STE12*alpha homolog is required for haploid filamentation but largely dispensable for mating and virulence in *Cryptococcus neoformans*. *Genetics.* **153**:1601–1615.
29. Wickes, B.L., Edman, U., and Edman, J.C. 1997. The *Cryptococcus neoformans* STE12alpha gene: a putative *Saccharomyces cerevisiae* STE12 homologue that is mating type specific. *Mol. Microbiol.* **26**:951–960.
30. D'Souza, C., et al. 2001. Cyclic AMP-dependent protein kinase controls virulence of the fungal pathogen *Cryptococcus neoformans*. *Mol. Cell. Biol.* **21**:3179–3191.
31. Hull, C.M., and Heitman, J. 2002. Genetics of *Cryptococcus neoformans*. *Annu. Rev. Genet.* **36**:557–615.
32. Collart, M. 2003. Global control of gene expression in yeast by the Ccr4-Not complex. *Gene.* **313**:1–16.
33. Erickson, T., et al. 2001. Multiple virulence factors of *Cryptococcus neoformans* are dependent on *VPH1*. *Mol. Microbiol.* **42**:1121–1131.
34. Tsegn-Rogenski, S.S., et al. 2003. Functional conservation of Dhh1p, a cytoplasmic DExD/H-box protein present in large complexes. *Nucleic Acid Res.* **31**:4995–5002.
35. Liu, H., et al. 1998. The NOT proteins are part of the *CCR4* transcriptional complex and affect gene expression both positively and negatively. *EMBO J.* **17**:1096–1106.
36. Coller, J., Tucker, M., Sheth, U., Valencia-Sanchez, M., and Parker, R. 2001. The DEAD box helicase, Dhh1p, functions in mRNA decapping and interacts with both the decapping and deadenylase complexes. *RNA.* **7**:1717–1727.
37. Maekawa, H., Nakagawa, T., Uno, Y., Kitamura, K., and Shimoda, C. 1994. The ste13 gene encoding a putative RNA helicase is essential for nitrogen starvation-induced G1 arrest and initiation of sexual development in the fission yeast *Schizosaccharomyces pombe*. *Mol. Gen. Genet.* **244**:456–464.
38. Sheth, U., and Parker, R. 2003. Decapping and decay of messenger RNA occur in cytoplasmic processing bodies. *Science.* **300**:805–808.
39. Akao, Y., et al. 1995. The rck/p54 candidate protooncogene product is a 54-kilodalton DEAD box protein differentially expressed in human and mouse tissues. *Cancer Res.* **55**:3444–3449.
40. Hata, H., et al. 1998. Dhh1p, a putative RNA helicase, associates with the general trancription factors Pop2p and Ccr4p from *Saccharomyces cerevisiae*. *Genetics.* **148**:571–579.
41. Maillet, L., and Collart, M. 2002. Interaction between Not1p, a component of the Ccr4-Not complex, a global regulator of transcription, and Dhh1p, a putative RNA helicase. *J. Biol. Chem.* **277**:2835–2842.
42. Valdes-Hevia, M.D., de la Guerra, R., and Gancedo, C. 1989. Isolation and characterization of the gene encoding phoshpoenolpyruvate carboxykinase from *Saccharomyces cerevisiae*. *FEBS Lett.* **258**:313–316.
43. Yin, Z., Smith, R.J., and Brown, A.J. 1996. Multiple signalling pathways trigger the exquisite sensitivity of yeast gluconeogenic mRNAs to glucose. *Mol. Microbiol.* **20**:751–764.
44. Kwon-Chung, K.J., Sorrell, T.C., Dromer, F., Fung, E., and Levitz, S.M. 2000. Cryptococcosis: clinical and biological aspects. *Med. Mycol.* **38**:205–213.

45. Lorenz, M., and Fink, G. 2001. The glyoxylate cycle is required for fungal virulence. *Nature.* **412**:83–86.
46. Body, B., Oneson, R., and Herold, D. 1987. Use of cerebrospinal fluid lactic acid concentration in the diagnosis of fungal meningitis. *Ann. Clin. Lab. Sci.* **17**:429–434.
47. Himmelreich, U., et al. 2003. Identification of metabolites of importance in the pathogenesis of pulmonary cryptococcoma using nuclear magnetic resonance spectroscopy. *Microbes Infect.* **5**:285–290.
48. Winzeler, E.A., et al. 1999. Functional characterization of the *Saccharomyces cerevisiae* genome by gene deletion and parallel analysis. *Science.* **285**:901–906.
49. Akhter, S., et al. 2003. Role of alternative oxidase gene in pathogenesis of *Cryptococcus neoformans*. *Infect. Immun.* **71**:5794–5802.
50. Huang, C., Nong, S., Mansour, M.K., Specht, C.A., and Levitz, S.M. 2002. Purification and characterization of a second immunoreactive mannoprotein from *Cryptococcus neoformans* that stimulates T-cell responses. *Infect. Immun.* **70**:5485–5493.
51. Levitz, S.M., Nong, S., Mansour, M.K., Huang, C., and Specht, C.A. 2001. Molecular characterization of a mannoprotein with homology to chitin deacetylases that stimulates T cell responses to *Cryptococcus neoformans*. *Proc. Natl. Acad. Sci. U. S. A.* **98**:10422–10427.
52. Kwon-Chung, K.J., and Bennett, J.E. 1992. *Medical Mycology.* Lea and Febiger. Philadelphia, Pennsylvania, USA. 866 pp.
53. Lazera, M.S., et al. 1996. Natural habitat of *Cryptococcus neoformans* var. *neoformans* in decaying wood forming hollows in living trees. *J. Med. Vet. Mycol.* **34**:127–131.
54. Bunting, L., Neilson, J., and Bulmer, G. 1979. *Cryptococcus neoformans*: gastronomic delight of a soil ameba. *Sabouraudia.* **17**:225–232.
55. Liu, L., Tewari, R.P., and Williamson, P.R. 1999. Laccase protects *Cryptococcus neoformans* from antifungal activity of alveolar macrophages. *Infect. Immun.* **67**:6034–6039.
56. Nosanchuk, J.D., Valadon, P., Feldmesser, M., and Casadevall, A. 1999. Melanization of *Cryptococcus neoformans* in murine infection. *Mol. Cell. Biol.* **19**:745–750.
57. Kojima, Y., et al. 1990. Cloning, sequence analysis and expression of ligninolytic phenoloxidase genes of the white-rot basidiomycete *Coriolus hirsutus*. *J. Biol. Chem.* **265**:15224–15230.
58. Myers, A., Pape, L., and Tzagoloff, A. 1985. Mitochondrial protein synthesis is required for maintenance of intact mitochondrial genomes in *Saccharomyces cerevisiae*. *EMBO J.* **4**:2087–2092.
59. Cox, G.M., Toffaletti, D.L., and Perfect, J.R. 1996. Dominant selection system for use in *Cryptococcus neoformans*. *J. Med. Vet. Mycol.* **34**:385–391.
60. Zolotukhin, S., Potter, M., Hauswirth, W.W., Guy, J., and Muzyczka, N. 1996. A humanized green fluorescent protein cDNA adapted for high level expression in mammalian cells. *J. Virol.* **70**:4646–4654.
61. Zhu, X., Gibbons, J., Garcia-Rivera, J., Casadevall, A., and Williamson, P.R. 2001. Laccase of *Cryptococcus neoformans* is a cell wall-associated virulence factor. *Infect. Immun.* **69**:5589–5596.
62. Liu, L., Wakamatsu, K., Ito, S., and Williamson, P.R. 1999. Catecholamine oxidative products, but not melanin, are produced by *Cryptococcus neoformans* during neuropathogenesis in mice. *Infect. Immun.* **67**:108–112.
63. Ausubel, F., et al. 2001. In situ hybridization to RNA. In *Current Protocols in Molecular Biology.* Volume 2. F. Ausubel et al., editors. John Wiley & Sons, Inc. New York, New York, USA. 14.3.1–14.3.6.
64. O'Neill, J., and Bier, E. 1994. Double-label in situ hybridization using biotin and digoxigenin-tagged RNA probes. *Biotechniques.* **17**:874–875.
65. Liu, H., Cottrell, T., Pierini, L., Goldman, W., and Doering, T. 2002. RNA interference in the pathogenic fungus *Cryptococcus neoformans*. *Genetics.* **160**:463–470.
66. Mondon, P., Chang, Y.C., Varma, A., and Kwon-Chung, K.J. 2000. A novel episomal shuttle vector for transformation of *Cryptococcus neoformans* with the ccdB gene as a positive selection marker in bacteria. *FEMS Microbiol. Lett.* **187**:41–45.
67. Tscharke, R., Lazera, M., Chang, Y., Wickes, B., and Kwon-Chung, K.J. 2003. Haploid fruiting in *Cryptococcus neoformans* is not mating type alpha-specific. *Fungal Genet. Biol.* **39**:230–237.
68. Toffaletti, D.L., and Perfect, J.R. 1997. Study of *Cryptococcus neoformans* actin gene regulation with a beta-galactosidase-actin fusion. *J. Med. Vet. Mycol.* **35**:313–320.